A portable fibre-probe ultraviolet light emitting diode (LED)-induced fluorescence detection system

Meas. Sci. Technol. **19** (2008) 025601 (8pp) doi:10.1088/0957-0233/19/2/025601

A portable fibre-probe ultraviolet light emitting diode (LED)-induced fluorescence detection system

Paul K Buah-Bassuah[1], Hubertus M von Bergmann[2], Ebenezer T Tatchie[1] and Christine M Steenkamp[2]

[1] Laser and Fibre Optics Centre, Department of Physics, University of Cape Coast, Cape Coast, Ghana
[2] Laser Research Institute, Department of Physics, University of Stellenbosch, Stellenbosch, South Africa

E-mail: buahbass@hotmail.com and hmvb@sun.ac.za

Received 11 July 2007, in final form 16 November 2007
Published 14 January 2008
Online at stacks.iop.org/MST/19/025601

Abstract
A portable fibre-probe fluorescence detection system comprising a continuous-wave high-power ultraviolet light emitting diode (UV LED) emitting at 365 nm as excitation source, a bifurcated fibre probe with a six-around-one fibre configuration to illuminate and read from a large target area (~3.6 mm^2) and an integrated PC-coupled spectrometer has been developed. The construction, calibration and operation of the fluorescence detection system are described. Demonstrative test measurements with the system for possible inspection of different ripening stages on some batches of horticultural and agricultural products (lemon, mandarin, banana leaf and ivy leaf) have been performed and results presented. The system is portable, comparatively low cost, easily operated and relative immune to ambient light, thus being suitable for field measurements.

Keywords: ultraviolet light emitting diode, plant fluorescence spectra, plant, integrated spectrometer

(Some figures in this article are in colour only in the electronic version)

1. Introduction

Fluorescence activity in biological samples is initiated when light of an excitation source is absorbed in the plant by light-harvesting chlorophyll protein complexes and the excitation energy is transferred to the reaction centres of the two photosystems (PSI and PSII) to be utilized for the occurrence of the photosynthetic reaction. A minor competing process of deactivation of excited chlorophyll pigments in the plant is the emission of chlorophyll fluorescence. Some studies of the plant chlorophyll fluorescence in relation to its photosynthetic activity tend to reveal a real correlation of the physiological status of the leaf or fruit in terms of its maturity and ripening process [1, 2]. The outlined principle is usefully applied in fluorescence detection systems for varied applications [3]. The operation of most of these existing fluorometers is therefore based on measuring the variation of emitted fluorescence spectral intensity of the sample under investigation as a function of fluorescence wavelength at a fixed excitation wavelength and varying time periods for given environmental conditions. With small size excitation sources, fibre probes and miniature-integrated spectrometers becoming commercially available during the last decade, better designs and construction of compact fluorescence detection systems have been explored to suit various applications in the study of plant growth, post-harvest losses of fruits, medicine and capillary electrophoresis [4–9]. To fulfil this objective, various successful attempts to build such systems for both laboratory and field measurements have been carried out, mainly by utilizing laser diodes and LED sources with different wavelengths extending from the violet to red spectral region. For instance, Mazzinghi [8] employed a red laser diode in his fluorosensor to monitor chlorophyll fluorescence in leaves using the time-dependent fluorescence peak ratio at

685/730 nm to evaluate the plant physiological status. The fluorescence emission in this case was limited to the red and infrared region because of the wavelength of the employed excitation source as well as the use of interference filters that select the detection band pass at specific peak wavelength of the filters [8]. However, the continuous complete spectra with pronounced peaks tend to be more versatile in analysing the fluorescence data instead of selection of dedicated multi-spectral band filters. More recently, the use of laser diode excitation sources in the ultraviolet region of the spectrum has made fluorescence emission from blue to near-infrared accessible and has been employed in plant as well as medical applications [6, 9]. These systems, though compact, require ultraviolet emitting laser diodes, which have low output power and are expensive (∼US $3000). In addition, laser diodes need precision alignment of a fibre port to the coupled fibre probe for optimum excitation signal. Recently, high-power LEDs emitting in the ultraviolet have become commercially available. Using LEDs as an alternative for laser diodes (LD) in some spectroscopic studies may have several advantages. Though both LED and LDs are small in size, LEDs have longer operating lifetimes, are stable, have reasonable input power requirements and are of low cost. They are available in a wide variety of emission wavelengths (ultraviolet to visible to infrared) and have broader emission bandwidths. The use of LED in fluorometers therefore offers an alternative and affordable system to ameliorate its functions for precision farming of fruits and crops. The UV LED used in the system as excitation light source costs approximately 30 times less than the conventionally employed UV LD.

Instruments employing LEDs with varied range of wavelength (290–950 nm) as excitation sources in a linear array configuration and coupled to micro lenses have been used for environmental monitoring of aerosols [10, 11]. The linear array configuration gives high optical output power, but results in a not very compact fluorescence detection system. Individual LEDs, on the other hand, have been successfully used to discriminate petroleum oils with important results [12]. In another example, a UV LED (wavelength 280 nm with pulsed output of a few μW) has been tested for its potential use in protein fluorescence studies [13]. LED-induced fluorescence detection systems for 2D electropherograms or phosphorescence measurements have been proposed [14]. In order to exploit some properties of LED excitation sources operating in pulse, modulation or continuous mode, Sipior [15] and Iwata [16] used phase modulation techniques in their fluorescence detection systems with promising results. Further, work exploring the luminescence properties of UV LED for time-resolved fluorescence found that luminescence is improved at higher injection current with specifically i-LED, operating at higher currents (600 mA). Relying on these developments, various factors have been considered to come up with an LED-induced fluorescence detection system that can effectively be employed to sense some differences in plant or fruit samples.

In this paper, a portable, continuous-wave UV LED fibre-probe fluorescence detection system is described. The system consists of a high-power UV LED excitation source emitting at

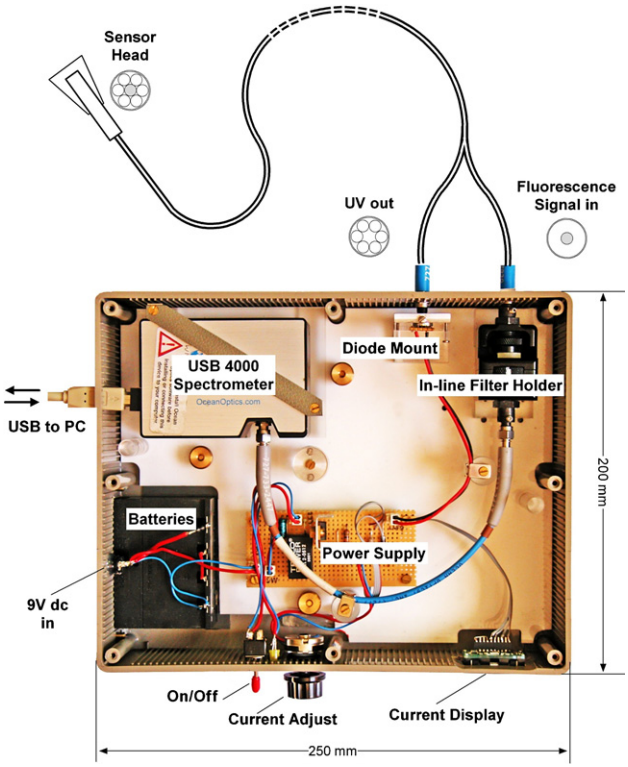

Figure 1. Layout of the UV LED fibre-probe fluorometer showing a photograph of the assembly of the device with the fibre probe.

365 nm, a fibre probe and a compact spectrometer to record the spectra. The employed LED excitation source has a nominal output power of 100 mW at a drive current of 500 mA but is limited to a value of approximately 30 mW by reducing the maximum drive current to 160 mA. The fibre probe consists of a Y-bifurcated fused silica fibre assembly made from 600 μm diameter quartz fibres. The system has been calibrated and tested on various plant samples to ascertain its potential uses and versatility of application. The use of a UV LED source in this system reduces cost to less than 10% for the excitation source compared to laser diodes and results in a total cost saving of almost 50% for the instrument. Employing an integrated spectrometer in the device coupled to a laptop computer offers a versatile system at a still affordable cost.

2. Instrumentation and fluorescence detection system setup

A photograph showing the layout of the UV LED fibre-probe fluorometer is shown in figure 1. The high-power UV LED source (Nichia Corporation, Model: NCU033-T) measuring 6.6 × 6.6 × 2.1 mm^3 has a peak wavelength of 365 nm with 8 nm spectral bandwidth and delivers a nominal maximum optical output power of 130 mW at operating voltage and current of 4.6 V and 500 mA, respectively, at an operating temperature of 25 °C. The UV LED source was soldered onto a small circuit board measuring 1 cm × 1 cm held in place by a metallic holder which provided sufficient cooling for the device at the maximum used operating current. It is driven

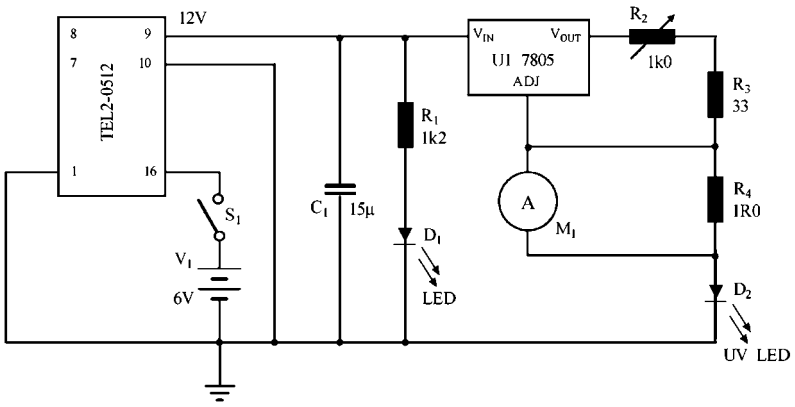

Figure 2. Circuit diagram for the UV LED driver.

by a stabilized constant-current power supply as shown in the circuit diagram in figure 2. The power supply has been designed to provide a maximum drive current of up to 160 mA for the LED and is fully adjustable over the current range using the potentiometer port. The operating current is displayed on an LCD display. By changing the forward current of the LED over the operating current range of 40–160 mA, the optical output power can be adjusted over the useful range with a maximum output of 27 mW. The power supply is powered by rechargeable batteries (4 × AA NiMH, 2000 mAh) sufficient for more than 10 h operation of the instrument.

A Y-shaped 2 m long bifurcated multimode optical fibre probe (Ocean Optics QBIF 600-UV-VIS) was employed assembled from individual cladded pure silica fibres with a core diameter of 600 μm and a NA of 0.22. The fibres are jacketed in a polyimide buffer resulting in an outside diameter 720 μm. The complete fibre bundle is contained in a chemically inert 6.35 mm outer Torlon body. One arm of the fibre assembly is made up from six 600 μm fibres and is coupled to the LED while the second arm with a single 600 μm fibre is connected to the spectrometer. The two arms of the fibre probe meet in a common leg combining the six fibres attached to the excitation source arranged closely packed coaxially around the central fibre connected to the spectrometer ensuring parallel orientation of all fibres. The ring of outer fibres in the common leg illuminates the sample while the central one collects or reads the emitted signal from the sample.

A number of different techniques have been evaluated for coupling the highly divergent light of the UV LED to the input of the fibre probe. The first technique consisted of focusing the LED output by either a single aspheric quartz lens (Thorlabs A390TM-A, $f_1 = 4.6$ mm with NA = 0.53, AR coated 350–600 nm) or a combination of two aspheric lenses and coupling it to the fibre bundle. A precision three-axis translation stage suited for micro-positioning was used for alignment and optimizing the coupling of the beam into a multimode fibre via an SMA connector. These arrangements did result in optimized coupling efficiencies of not more than 1%. A significantly improved coupling was achieved by simple 'butt-coupling' the LED to the fibre input. In this arrangement, the fibre is placed in close proximity (approximately 0.5 mm) of the output window of the LED. Sufficient alignment accuracy is obtained by a fixed holder with clamping screws, significantly reducing complexity and cost of the coupling arrangement. A maximum of 1.67 mW of power was measured at the fibre output for an input power of 27.2 mW corresponding to a coupling efficiency of 6.1%. Although the coupling efficiency is low, the output still compares favourably to UV LDs and can, if necessary, still be increased by raising the drive current of the LED within the allowed operating regime of the LED. The present output was found to be more than adequate for the present experiments.

The central core fibre of the common leg that reads the information diverges from the breakout of the common end of the assembly to form the one arm of the fibre which is coupled by an SMA connector to an in-line filter holder (Ocean Optics, 74-ACH FHS-UV) inside the fluorescence detection system housing. The filter holder contains two collimating lenses (74-UV, $f = 10$ mm and 5 mm diameter) arranged before and after a flat optical long-pass filter (Ocean Optics, OF2-GG395) projecting the collimated light from the sample. The long-pass filter passes the sample fluorescence >400 nm and rejects the UV excitation light backscattered into the probe fibre. The lenses in the filter holder have inner barrels and threaded SMA 905 connectors for fibre coupling. The inner barrel slides relative to the lens fixture for adjusting the lens focus while a set screw secures the barrel adjustment from converging to diverging field of view. A short multimode single fibre with 600 μm core connects the filter holder to the SMA connector of the PC-coupled miniature spectrometer (Ocean Optics, USB 4000FL). The spectrometer directly plugs into the USB port of a laptop PC, thus eliminating any additional A/D interface and also draws its power through the USB connection. The spectrometer is equipped with a 100 μm slit and a grating of 600 lines mm^{-1} that disperses the light in the spectral range of 300–1000 nm capturing it on a 3648 element CCD detector. A spectral resolution of 8 nm is obtained which is adequate for horticultural as well as most spectroscopic applications. The UV LED output beam from the fibre induces the sample for the emission of the fluorescence signal which is collected by the single fibre into the spectrometer. A small aluminium funnel cap is placed on the common leg of the fibre that can be moved up and down close enough to the sample to concentrate

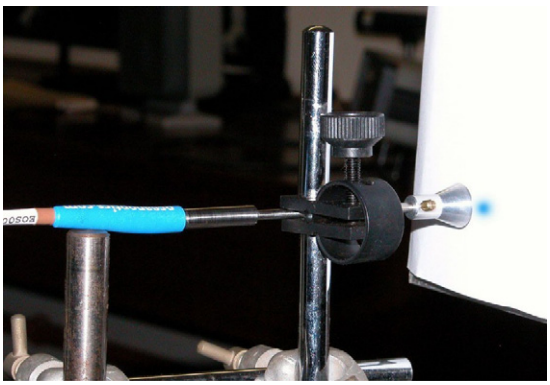

(*a*)

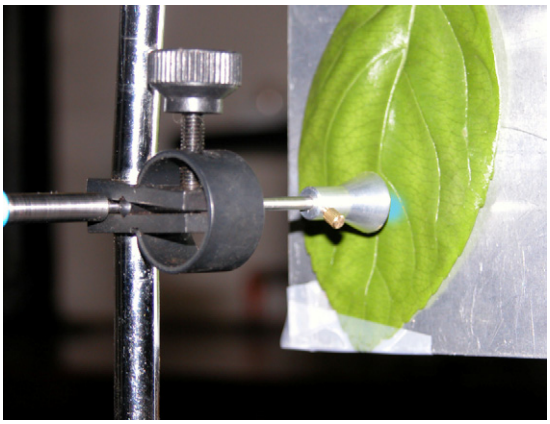

(*b*)

Figure 3. Experimental set-up for (*a*) the blue fluorescence of the white paper sample at the target and (*b*) measurement of fluorescence on a leaf.

and collect the fluorescence signal while blocking off ambient light. The complete fluorescence detection system is enclosed in a small moulded plastic case measuring 200 × 250 × 65 mm^3 and connects to a bifurcated fibre probe as shown in figure 1. Figure 3 shows photographs of the experimental set-up for (*a*) a fluorescing paper sample for calibration of the system and (*b*) for measurements of leaves or fruits.

3. Measurements

The spectrometer is controlled by data acquisition and display software (Ocean Optics SpectraSuite, OOI Base32 Vers. 2) which permits complete control over data acquisition, data processing and rendering. Further analysis of the data in graphical representations is imported into scientific graphing and data analysis software (Origin Vers. 6). The sensitivity of the instrument can be changed according to the emitted sample signal by adjusting the integration period which has a linear relationship to the sensitivity. A calibration was performed using a 200 W calibrated quartz tungsten/halogen lamp (Oriel 63355) with a known spectral profile. The reference spectrum was recorded through the optical fibre. In addition, a possible fluorescence contribution from the optical fibre to the measured signal has been excluded by measuring

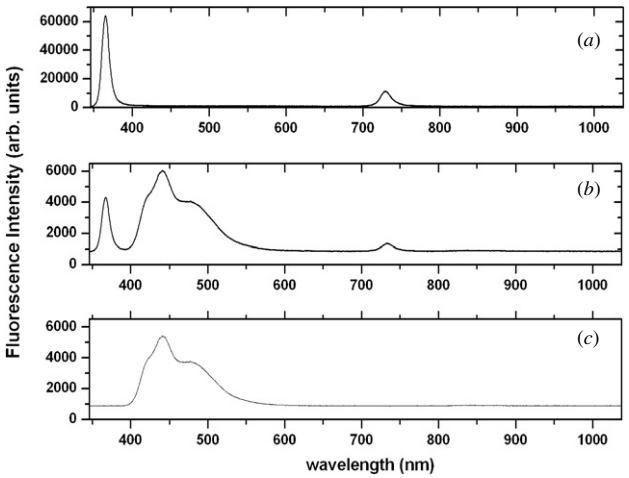

Figure 4. Fluorescence spectra illustrating (*a*) the UV LED diode, (*b*) UV LED beam on the white paper target and (*c*) white paper using the long-pass filter as a means of explaining the measurement procedure of the system and suppressing the fluorescence from the LED source. There is no fluorescence from the fibre probe.

the back-reflected signal from a plane polished aluminium plate as a sample target. The UV LED of the fluorescence detection system was operated at a forward current of 100 mA. The area illuminated on the target by the fibre probe was 3.6 mm^2 and the induced fluorescence signal from the sample received through the single core of the other optical fibre was measured to have an optical output power of 500 μW. The recorded signal that was reflected from the aluminium plate and recorded by the spectrometer using an integration time of 100 μs gives the LED emission peak at 365 nm with spectral bandwidth as well as a second emission peak at the second-order position of the spectrometer of 729 nm. It is evident that there is no contribution to the spectrum from either the fibre or the target plate. By inserting a long-pass interference filter (>400 nm) in the filter holder the LED emission at 365 nm and the second-order peak at 729 nm are suppressed so as not to interfere with the Stokes-shifted fluorescence signal.

In order to demonstrate this concept and test the fluorescence detection system, white writing paper was placed on the aluminium plate as sample and the paper fluorescence was recorded first without the filter at an integration time of 400 ms and also with the filter inserted at the same integration time as found in the literature. It can be observed that a significantly longer integration time is needed to record the fluorescence signal. The signal-to-noise ratio was improved by first subtracting the background noise. This is achieved by first recording the dark current without the sample before recording the fluorescence signal. Figure 4(*c*) demonstrates the use of a long-pass filter in the fluorescence detection arm of the fibre probe to suppress the LED emission. This enables the fluorescence signal of the sample under test to be measured and it also ascertains the absence of fluorescence of the fibre probe during the measurement thus demonstrating a calibration of the measurement procedures for the device. Processing of the detected signal is done by the software which automatically subtracts the dark current and displays the averaged sample

Table 1. Fluorescence peak position and peak intensity (PI) for plant materials. PI with subscript represents the spectra colour (B—blue, GR—green, Y—yellow, R—red and FR—near-infrared).

Fruit/leaves		Peak position (nm)	Peak intensity (au)
Mandarin (a) (greenish-orange skin)	PI_{GR}	494.01	9636.52
	PI_{Y}	552.89	8169.99
	PI_{R}	691.66	3963.30
	PI_{FR1}	744.33	3448.03
	PI_{FR2}	792.73	3408.39
Mandarin (b) (yellowish-orange skin)	PI_{GR}	494.01	5630.65
	PI_{Y}	584.42	6383.73
	PI_{R}	693.77	3725.48
	PI_{FR1}	744.23	3210.22
	PI_{FR2}	792.73	3249.85
Mandarin (c) (orange skin)	PI_{GR}	494.01	6700.82
	PI_{Y}	565.51	9200.53
	PI_{R}	693.77	4042.57
	PI_{FR1}	744.23	3329.13
	PI_{FR2}	792.73	3804.76
Lemon (a) (greenish-yellow skin)	PI_{GR}	515.94	43 654.53
	PI_{R}	683.94	7027.99
	PI_{FR1}	740.67	18 290.03
	PI_{FR2}	795.45	5034.71
Lemon (b) (yellow skin)	PI_{GR}	533.39	6564.17
	PI_{FR2}	791.58	6570.55
Ivy leaf	PI_{B}	442.61	3297.29
	PI_{GR}	531.92	3825.90
	PI_{R}	686.19	6296.69
	PI_{FR}	735.17	5294.28
White writing paper	PI_{B1}	440.84	5461.49
	PI_{B2}	478.43	3758.04

signal. Figure 3(*a*) shows a photograph of the experimental set-up used and the blue fluorescence of the white paper sample used as a target.

Measurements were then extended to living plant material examining leaves of banana and ivy plants. The leaves were placed in front of the fibre probe and were supported from the back by a small aluminium plate as shown in figure 3(*b*). Fluorescence signals of the plant leaves were recorded for integration times varied between 1 and 2 s using the long-pass filter in the filter holder and confirm the spectral signal as found in [9]. The band pass spectra at specific wavelengths extracted from these spectra are shown in table 1. Two types of fruit, mandarins and lemons of varied colouration, were also investigated to demonstrate some properties of the ripening process. In this experiment, three sample batches of mandarins from the same tree but with different colouration (ten each of greenish-orange, yellowish-orange and orange skin) as well as two sample batches of lemons with different colouration (ten each of greenish-yellow and yellow skin) were placed in turn on a target table, recording the Stokes-shifted fluorescence signal of the fruits. Integration times varying between 4 and 6 s had to be used to probe the skin of the fruits for their respective spectral output. The objective and motivation of the experiment was to demonstrate the ability of immediate inspection and assessment of fruit and at the same time investigating the various ripening stages of different types

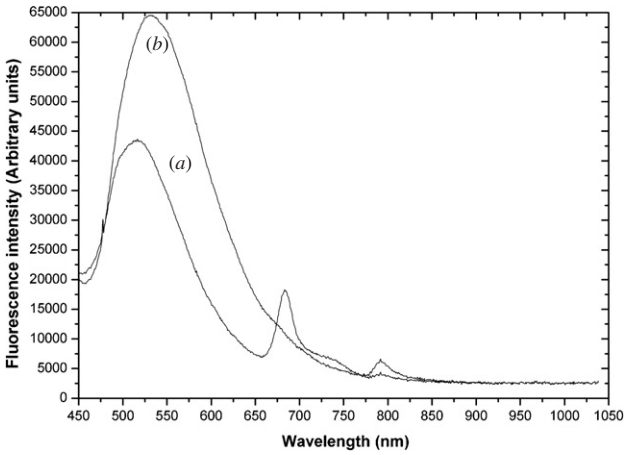

Figure 5. Fluorescence spectra of lemon skin showing (*a*) greenish-yellow skin lemon and (*b*) yellow skin lemon.

of fruit. In a further preliminary study some batches of fruits, selected off the shelf in two supermarkets, were investigated over a period of weeks. Fruits were stored at a room temperature of 22 °C and fluorescence spectra were recorded at different locations of the fruit (head, side and tail) over a period of time in order to understand the possible post-harvest losses resulting from stress condition during the ripening process under the given ambient conditions. The results of such studies carried out with the fluorescence detection system provided a further understanding of the ripening process of fruit.

4. Results and discussion

Using the software's image processing features of smoothing and averaging on the fluorescence signal imported from the Ocean Optics SpectraSuite software results in the typical spectra shown in figures 4–6. Figures 5(*a*) and (*b*) show spectra of greenish-yellow and yellow lemon skins, respectively. It is observed that a change in colouration implies the variation of chlorophyll content and physiological status of the lemon and the consequent ripening process. In figure 5(*a*), the skin of the lemon was greenish-yellow and the spectrum shows a dominant yellow fluorescence signal with the red and near-infrared peaks also evident. As the colouration of the skin intensifies from greenish-yellow to pure homogenous yellow, the spectra then change as shown in figure 5(*b*) with the red and near-infrared peaks reducing considerably and almost vanishing in height. The ripening process contributes to the reduction in chlorophyll content and as a result serves as an environmental stress factor. Figures 6(*a*) to (*c*) show fluorescence spectra recorded from the skin of a greenish-orange, a yellowish-orange and an orange mandarin, respectively. In figure 6(*a*) the greenish-orange skin exhibits a strong peak at 500 nm with smaller peaks in the orange range of the spectrum. Figure 6(*b*) shows a smaller green peak as compared to the orange peak while in figure 6(*c*) a very high orange peak signifies the ripening colouration of the fruit.

Table 2. Fluorescence peak intensity ratio data for various samples such as white writing paper, fruit and leaf. The various intensity ratios for the two wavelengths are indicated below. The calculated ratios and their errors (in brackets) show the trends of fluorescence signals in the different samples.

Materials	Mandarin A	Mandarin B	Mandarin C	Lemon	Ivy leaf	White writing paper
Fluorescence peak intensity ratio/error	F494/F552 1.18 (0.02)	F494/F584 0.88 (0.01)	F494/F565 0.72 (0.01)	– –	F442/F531 0.81 (0.01)	F440/F478 1.45 (0.01)
	F494/691 2.43 (0.02)	F494/F693 1.51 (0.02)	F494/F693 1.65 (0.02)		F442/686 0.52 (0.01)	
	F691/F744 1.14 (0.01)	F693/F744 1.16 (0.02)	F693/F744 1.21 (0.01)	F683/F740 2.60 (0.02)	F686/F735 1.17 (0.01)	

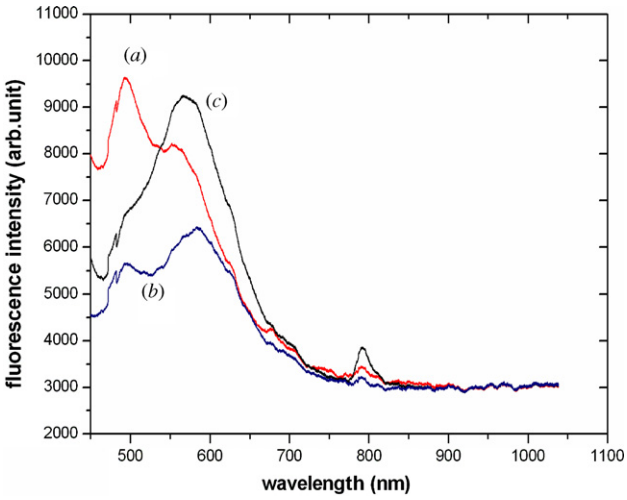

Figure 6. Fluorescence spectra of mandarin skin showing (*a*) greenish-orange, (*b*) yellowish-orange and (*c*) orange skin mandarin.

The resulting peak intensities with their corresponding wavelengths are shown in table 1. From table 1, the leaf demonstrates different chlorophyll concentration by examining the ratio of the peak intensities [6]. Such observations can be used to monitor plant growth as well as stress in plants. The spectrum reveals fluorescence peaks in the blue/green region F442/F531 and two pronounced peaks at 690 nm and 735 nm attributed to the chlorophyll fluorescence. The ratio of F691/F735 shows the chlorophyll status in the plant, while F442/F531 reflects not only the chlorophyll but also pigmentation of green leaves, which can be used as an additional fluorescence parameter to judge the physiological and pigment status of the plant. An investigation of the variation of these parameters is therefore useful as a means to understand the growth processes of the plant and to assess various stress conditions [18, 19]. The wavelength region around 440 nm called the blue fluorescence and around 494–533 nm called the green fluorescence is derived from the products of the plant's secondary metabolism such as ferulic acid derivatives, phenyl propanoids and partially mesophyll origin and tends to be a proper index of a plant's health and stress. The spectra at the peak of 740 nm (far red fluorescence) and that of 690 nm (red fluorescence) are also good indicators to evaluate chlorophyll concentration [20, 21]. Any increase in the blue or green fluorescence shows stress on the leaf of the plant or on the fruit. Any decrease of the peak of the far-red fluorescence 740 nm indicates an inactive photosynthesis process, and thus the plant leaf or fruit can be better assessed by the plant physiological status during the ripening process. With the 690 nm and 740 nm fluorescence peak spectra, it can be found that the fluorophore present in leaf or fruit can be used to describe the chlorophyll degradation during the photosynthetic process. The calculated fluorescence peak ratios for the blue/green, blue/red and red/far-red peaks derived from the different samples are shown in table 2 with an estimated error of 1%. The observation of the variation of the fluorescence signal ratios for the three different batches of mandarin harvested from the same tree demonstrates the progress of the ripening process and the maturity of the fruit. The spectra of the greenish-yellow lemon demonstrate the presence of chlorophyll fluorescence as evident in figure 6(*a*). By observing the behaviour of the intensities of the fluorescence signals or the ratios of the different fluorescence peaks, the important role of the photosynthetic activity due to the reaction centres in the two photosystems (PSI and PSII) can be demonstrated. The measured spectral fluorescence signatures of these fruits at different sides sensitively show up differences in both fruit ripening development and maturity stage. In addition, such fluorescence signatures serve as good and very useful indicators of the physiological status of leaves and of various plant performances [5]. In table 2, the fluorescence ratio of green/red shows a decrease from mandarin A to C while the red/far-red fluorescence ratio increases from mandarin A to C. The fluorescence ratio of lemon is higher than that of mandarin which demonstrates the amount of chlorophyll present in the different fruits. In order to examine the ripening process, it will be appropriate to restrict oneself to the red/far-red fluorescence ratio to assess the trend of chlorophyll degradation in the course of the ripening process over a period of time. The blue/green and red/far-red ratios relate to the variation of the acidic and chlorophyll content in the plant growth or maturity processes. These observations tend to reinforce the fact that storage under room temperature conditions serves as a stress factor on the ripening process of fruits. Further investigations were carried out by monitoring the chlorophyll fluorescence of fruit stored at room temperature over an extended period of time. The peaks at red (690 nm) and near-infrared (730 nm) were recorded at regular intervals for each side of the fruits. Fruit samples

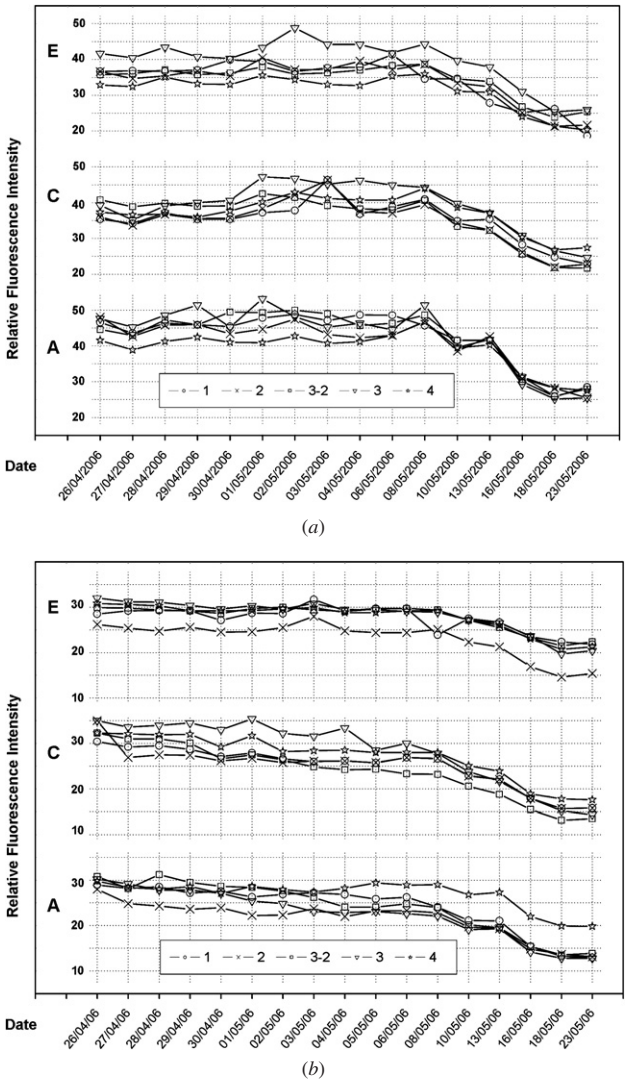

Figure 7. Fluorescence spectra for lemon (fruits A, C, E) for a period of 5 weeks. Numbers 1, 3, 3-2 represent the skin sides of the fruits while 2 and 4 are the head and tail ends of the lemon, respectively. (*a*) Fluorescence spectra at 690 nm in the presence of daylight L. (*b*) Fluorescence spectra at 730 nm in the presence of daylight L.

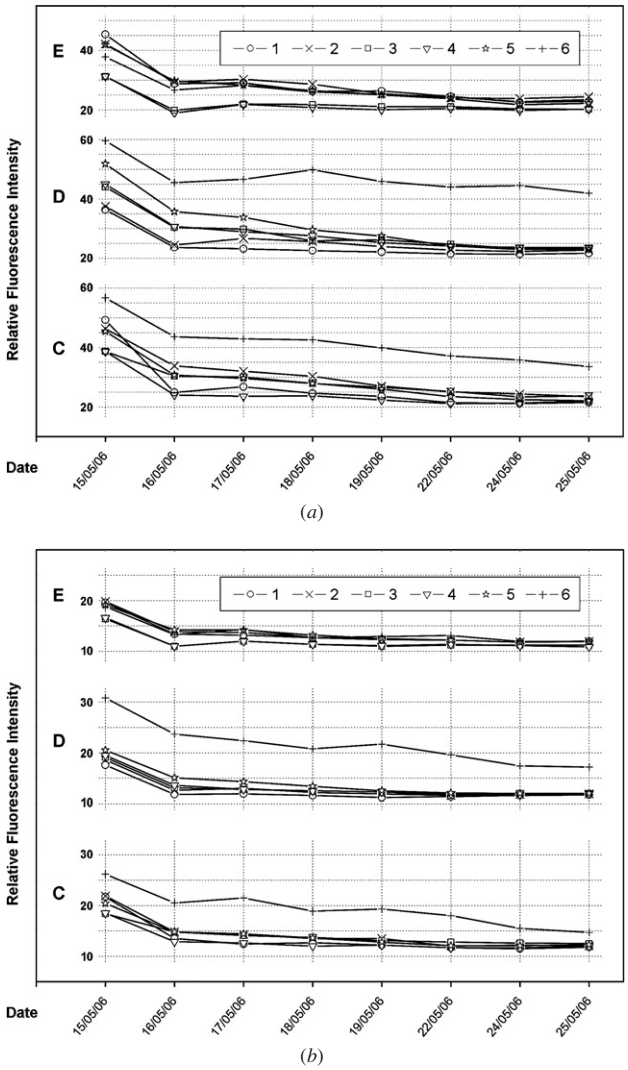

Figure 8. Fluorescence spectra for mandarin (fruits C, D, E) for a period of 10 days. Numbers 1, 2, 3, 4 represent the skin sides of the fruits while 5 and 6 are the head and tail ends of the mandarin, respectively. (*a*) Fluorescence spectra at 690 nm in the presence of daylight L. (*b*) Fluorescence spectra at 730 nm in the presence of daylight L.

such as lemon and mandarin were used. With the lemon fruit, the numbers 1, 3, 3-2 represent skin sides of the fruit while 2 and 4 represent the head and the tail end of the fruit, respectively. In the case of the mandarin, 1, 2, 3, 4, represent the skin sides while 5 and 6 represent the head and the tail end, respectively. Figures 7 and 8 show fluorescence spectra of lemon and mandarin at wavelengths of 690 nm and 730 nm recorded over a period of 5 weeks and 10 days, respectively. In figure 7, the chlorophyll fluorescence intensities of the lemons vary steadily with time and drastically reduce in the fourth week while in figure 8 the chlorophyll fluorescence intensities of the mandarins sharply reduce in the first week and steadily diminish for the rest of the measurements. The chlorophyll fluorescence was also found to be higher at the head and tail ends of the fruit. In the fifth storage week under room temperature conditions the lemon skin began to harden and change colour.

5. Conclusion

A portable continuous-wave ultraviolet fibre-probe UV LED-induced fluorescence detection system has been developed. The fluorescence detection system has been tested on various plant materials. Employing the system for fluorescence measurements on fruit and leave samples for a given time, it has been demonstrated that the distinct chlorophyll fluorescence response serves as a useful indicator that can help to understand the photosynthetic apparatus relating to the different stages of chlorophyll degradation during the ripening process. It is being used as a means of sorting out the fruit coloration

based on the presence of chlorophyll fluorescence derived from the peak intensity ratios. The system looks very promising for both horticultural and agricultural applications where post-harvest monitoring becomes paramount and the ripening process relies on the environmental factors such as room and storage temperatures. It is also essential to follow growth patterns of various breeding crops till harvest time under the influence of certain stress conditions using the system. The system employs a number of novel concepts simplifying the construction and reducing costs. Employing low cost high-power UV LEDs instead of the conventionally used UV laser diodes has resulted in a significant cost reduction (∼50%) while at the same time giving similar, if not better, performance of the instrument. The use of a bifurcated fibre probe results in an all-fibre construction eliminating the need for fibre ports, beam splitters and sensitive instrument adjustments. The reduced cost will be of particular importance for the intended employment of the instrument on the African continent and in other less developed countries.

Acknowledgments

PKB-B and ET-T are most grateful to the African Laser Centre (ALC) and the National Laser Centre (NLC), Pretoria, South Africa, for sponsoring this project at the University of Stellenbosch in terms of equipment and their fellowships. PKB-B is also grateful to Professor Sune Svanberg of Lund Institute of Technology, Sweden, for first introducing him to fluorometers under the Upssala University IPPS Programme. We are also grateful to the Laser Research Institute (LRI) of the University of Stellenbosch for hosting us and the University of Cape Coast, Ghana, for releasing us for this collaborative work in South Africa. We acknowledge J Burns for providing the constructed mechanical parts as well as P Fourie for building the stable constant current driver for the fluorescence detection system. We also acknowledge Nichia Corporation (Branch in Germany) for giving us free samples of the LEDs for our detection system.

References

[1] Lakowicz J R 1999 *Principles of Fluorescence Spectroscopy* 2nd edn (New York: Plenum)

[2] Baker N R and Rosenqvist E 2004 Applications of chlorophyll fluorescence can improve crop production strategies: an examination of future possibilities *J. Exp. Biol.* **55** 1607–21

[3] Capelle G A and Franks L A 1979 Laboratory evaluation of two laser fluorosensor systems *Appl. Opt.* **18** 3579–86

[4] Nedbal L, Soukupova J, Kaftan D, Whitmarsh J and Trtilek M 2000 Kinetic imaging of chlorophyll fluorescence using modulated light *Photosynth. Res.* **66** 3–12

[5] Herold B, Truppel I, Zude M, Herppich W B and Geyer M 2005 Monitoring the fruit development on tree by a portable spectrophotometer *Acta Hort.* **687** ISHS 361–2

[6] Anderson B, Buah-Bassuah P K and Tetteh J P 2004 Using violet laser-induced chlorophyll fluorescence emission spectra for crop yield assessment of cowpea (*Vigna unguiculata (L) Walp*) varieties *Meas. Sci. Technol.* **15** 1255–65

[7] Chang Y, Shih C and Lin C 2006 UV light-emitting diode-induced fluorescence detection combined with online sample concentration techniques for capillary electrophoresis *J. Soc. Anal. Chem.* **22** 235–40

[8] Mazzinghi P 1996 A laser fluorometer for field measurements of the F685/F730 chlorophyll fluorescence ratio *Rev. Sci. Instrum.* **67** 3737–44

[9] Gustafsson U, Palsson S and Svanberg S 2000 Compact fiber-optic fluorosensor using a continuous-wave violet diode laser and an integrated spectrometer *Rev. Sci. Instrum.* **68** 2666–70
Chappelle E W, Wood F M, Newcomb W W and McMurtny 1985 Laser-induced fluorescence of green plants *Appl. Opt.* **24** 74–80
Ndao A S, Konte A, Biaye M, Faye M E, Faye N A B and Wague A 2005 Analysis of chlorophyll fluorescence spectra in some tropical plants *J. Fluorescence* **15** 123

[10] Davitt K, Song Y, Patterson W R III, Nurmikko A V, Gherasimova, Han J, Pan Y and Chang R K 2005 290 and 340 nm UV LED arrays for fluorescence detection from single airborne particles *Opt. Exp.* **13** 9548–55

[11] Pan Y, Boutou V, Chang R K, Ozden I, Davitt K and Nurmikko A V 2003 Application of light emitting diodes for aerosol fluorescence detection *Opt. Lett.* **28** 1707–9

[12] Rostampour V and Lynch M J 2006 Quantitative techniques to discriminate petroleum oils using LED-induced fluorescence *WIT Trans. Ecol. Environ. Water Pollut. VIII: Modelling Monit. Manage.* **95** 255

[13] McGuiness C D, Sagoo K, McLoskey D and Birch D J S 2004 A new sub-nanosecond LED at 280 nm: application to protein fluorescence *Meas. Sci. Technol.* **15** L19–L22

[14] Arraez-Roman D, Fernandez-Sanchez J F, Cortacero-Ramirez S, Segura-Carretero A and Fernandez-Gutierrez A 2006 A simple light-emitted diode-induced fluorescence detector using optical fibers and a charge coupled device for direct and indirect capillary electrophoresis methods *Electrophoresis* **27** 1776–83

[15] Sipior J, Carter G M, Lakowicz J R and Rao G 1997 Blue light-emitting diode demonstrated as an ultraviolet excitation source for nanosecond phase-modulation fluorescence lifetime measurements *Rev. Sci. Instrum.* **68** 2666–70

[16] Iwata T, Kamada T and Araki T 2000 Phase-modulation fluorometer using an ultraviolet light-emitting diode *Opt. Rev.* **7** 495–8

[17] Jin D, Connally R and Piper J 2006 Long-lived visible luminescence of UV LEDs and impact on LED excited time-resolved fluorescence applications *J. Phys. D: Appl. Phys.* **39** 461–5 and all references therein

[18] Subhash N and Mohanan C N 1995 Remote detection of nutrient stress in groundnut plants by deconvolution of laser-induced fluorescence *Spectra Proc. Int. Geoscience and Remote Sensing Symp. (Firenze)* vol 3 pp 2323–5

[19] Lichtenthaler H K 1990 Applications of chlorophyll fluorescence in stress physiology and remote sensing *Applications of Remote Sensing in Agriculture* ed M Steven and J A Clark (London: Butterworth Scientific) pp 287–305

[20] Cerovic Z G, Samson G, Morales F, Tremblay N and Moya I 1999 Ultra violet induced fluorescence for plant monitoring: present state and prospects *Agronomie* **19** 543–78

[21] Saito Y, Matsubara T, Koga T, Kobayashi F, Kawahara T D and Nomura A 2005 Laser-induced fluorescence imaging of plants using liquid crystal tunable filter and charged coupled device imaging camera *Rev. Sci. Instrum.* **76** 106103